Strong coupling superconductivity and prominent superconducting fluctuations in the new superconductor $Bi_4O_4S_3$

LI Sheng[1], YANG Huan[1,†], FANG DeLong[1], WANG ZhenYu[2], TAO Jian[1], DING XiaXin[1], and WEN HaiHu[1,*]

[1]*Center for Superconducting Physics and Materials, National Laboratory of Solid State Microstructures and Department of Physics, Nanjing University, Nanjing 210093, China* and

[2]*National Laboratory for Superconductivity, Institute of Physics and National Laboratory for Condensed Matter Physics, Chinese Academy of Sciences, Beijing 100190, China*

Electric transport and scanning tunneling spectrum (STS) have been investigated on polycrystalline samples of the new superconductor $Bi_4O_4S_3$. A weak insulating behavior in the resistive curve has been induced in the normal state when the superconductivity is suppressed by applying a magnetic field. Interestingly, a kink appears on the temperature dependence of resistivity near 4 K at all high magnetic fields above 1 T when the bulk superconductivity is completely suppressed. This kink associated with the upper critical field as well as the wide range of excess conductance at low field and high temperature are explained as the possible evidence of strong superconducting fluctuation. From the tunneling spectra, a superconducting gap of about 3 meV is frequently observed yielding a ratio of $2\Delta/k_B T_c \approx 16.6$. This value is much larger than the one predicted by the BCS theory in the weak coupling regime ($2\Delta/k_B T_c \approx 3.53$), which suggests the strong coupling superconductivity in the present system. Furthermore, the gapped feature persists on the spectra until 14 K in the STS measurement, which suggests a prominent fluctuation region of superconductivity. Such superconducting fluctuation can survive at very high magnetic fields, which are far beyond the critical fields for bulk superconductivity as inferred both from electric transport and tunneling measurements.

Superconductivity is induced by quantum condensation of a large number of paired electrons. The pairing is supposed to be established between the two electrons with opposite momentum and spins by exchanging the phonons. According to the Bardeen-Cooper-Schrieffer (BCS) theory, a linear relationship between the electron pairing gap Δ and superconducting (SC) critical temperature T_c, i.e., $2\Delta/k_B T_c = 3.53$ exists in the weak coupling regime. In recent years, the original proposal about the pairing based on the electron-phonon coupling has been gradually replaced by the more exotic pairing mechanism, such as through exchanging the magnetic spin fluctuations, and T_c can be increased to a higher level. The SC pairing mechanism of the cuprates[1] and the iron pnictides[2], although not yet being settled down completely, should have a close relationship with strong correlation effect. In cuprates[3] and pnictides[4], the ratio $2\Delta/k_B T_c$ is generally much larger than that predicted by the weak coupling BCS theory, implying the strong coupling superconductivity (in some conventional BCS superconductors, like Pb, Hg and PbBi, the coupling is also strong[5]). Another important issue for cuprates is that the electron correlation in the normal state may induce strong superconducting fluctuation which has been widely investigated[6–10]. However, the fluctuation region in iron pnictides seems not that wide[11,12]. SC fluctuation was used to be associated with another characteristic property, the so-called pseudogap effect in cuprates[13]. However the SC fluctuation temperature was proved to be different from the pseudogap temperature by further experiments[14,15]. Although pseudogap has a very close

relationship with superconductivity, there is however no consensus yet on the origin of it in cuprates. The scanning tunneling spectra show a continuous evolution from the SC gap feature to the pseudogap feature which exists at temperatures far above T_c[16]. High-T_c superconductivity should have a close relationship with the correlation effect of electrons from the 3d orbitals[17–19]. In the heavy Fermion systems[20] and organic materials[21], a similar conclusion may be achieved. In this regard, it is natural to explore new superconductors with possible higher transition temperatures in compounds with transition metal elements in which the electron correlations could be strong. The electrons in the p-orbital, especially those from the 5p or 6p orbits, are normally assumed to have weak repulsive potential and quite wide band width, and hence have very weak correlation effect. It would be surprising to find out superconductivity with exotic feature in the p-orbital based compounds.

Recently, Mizuguchi et al.[22] discovered superconductivity with $T_c^{\mathrm{onset}} = 8.6$ K (determined from the point where resistivity deviates from the linear extrapolation of normal-state value) and $T_c^{\mathrm{zero}} = 4.5$ K in the so-called BiS_2 based compound $Bi_4O_4S_3$. This compound has a layered structure with the space group of I4/mmm or I-42m. Shortly the same group reported superconductivity at about 10.6 K in another system $LaO_{1-x}F_xBiS_2$ by doping electrons into the material through substituting oxygen with fluorine[23]. By replacing the La with Nd or Ce, other new BiS_2 based materials were reported[24,25]. Quickly followed is the theoretical work based on the first principles band structure calculations[26], which predicts

that the dominating bands for the electron conduction as well as for the superconductivity are derived from the Bi $6p_x$ and $6p_y$ orbits. In this paper, we present a set of data for an intensive study on the transport and scanning tunnelling spectroscopy (STS) measurements of the new superconductor $Bi_4O_4S_3$. Our results clearly illustrate the strong coupling superconductivity and prominent superconducting fluctuation in this interesting superconductor.

I. EXPERIMENTS

The polycrystalline samples were synthesized by using a two-step solid state reaction method. Firstly, the starting materials bismuth powder (purity 99.5%, Alfa Aesar) and sulfur powder (purity 99.99%, Alfa Aesar) were mixed in a ratio of 2:3, ground and pressed into a pellet shape. Then it was sealed in an evacuated quartz tube and followed by annealing at $500\,°C$ for 10 hours. The resultant pellet was smashed and ground together with the Bi_2O_3 powder (purity 99.5%, Alfa Aesar) and sulfur powder, in stoichiometry as the formula $Bi_4O_4S_3$. Again it was pressed into a pellet and sealed in an evacuated quartz tube and burned at $510\,°C$ for 10 hours. Then it was cooled down slowly to room temperature. The second step was repeated in achieving good homogeneity. The resultant sample looks black and very hard. We cut the sample and obtained a specimen with a rectangular shape for the resistive measurements. The resistivity was measured with Quantum Design instrument PPMS-16T. The temperature stabilization was better than 0.1% and the resolution of the voltmeter was better than 10 nV. The magnetization was detected by the Quantum Design instrument SQUID-VSM with a resolution of about 5×10^{-8} emu. The sample was shaped as a bar with a typical size of $2mm \times 2mm \times 0.5mm$ for the STS measurements. Since the sample is very hard, which allows us to polish the sample surface and obtain a shiny and mirror-like surface. The top surface was polished by sandpapers with different grit sizes (smallest of ISO P10000). The tunnelling spectra were measured with an ultra-high vacuum, low temperature and high magnetic field scanning probe microscope USM-1300 (Unisoku Co., Ltd.). In STS measurements, Pt/Ir tips were used. The set points of the bias voltage and tunneling current are 40 mV and 100 pA respectively to fix the tip height in topographic mode. Then the differential conductivity was recorded while the bias voltage was swept with the tip held at a fixed vertical distance with z -piezo-feedback off for the STS measurements. There is no atomically resolved topography measured on the sample since it is a polycrystalline one. The roughness of the surface for STS measurements is about 2 nm, while on some flat surface of a grain the roughness is about 0.5 nm locally. The STS spectra are repeatable at different positions in one grain. In reducing noise of the differential conductance spectra, a lock-in technique with an ac modulation of 0.1 mV at
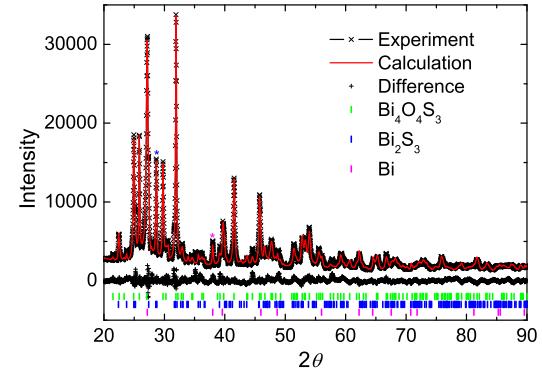

FIG. 1: (color online) The XRD pattern (symbols) of $Bi_4O_4S_3$ refined (red solid lines) by Topas (Bruker-D8). It is clear that the main phase is $Bi_4O_4S_3$ containing Bi_2S_3 impurity marked by a blue star and Bi by a red star. The ratio among the three phases $Bi_4O_4S_3$:Bi_2S_3:Bi is about 80:15:5.

987.5 Hz was typically used.

II. RESULTS

The crystallinity of the sample was checked by x-ray diffraction (XRD) with the Brook Advanced D8 diffractometer with Cu Kα radiation. The analysis of XRD data was done by the softwares Powder-X and Topas. The XRD pattern looks very similar to that reported by Mizuguchi et al.[22]. The result of Rietveld fitting was done with the Topas program in Fig. 1, yielding a 80% volume of $Bi_4O_4S_3$ with 20% of impurities which are mainly Bi_2S_3(15%) and Bi(5%).

In Fig. 2(a) we present the temperature dependence of resistivity measured at three magnetic fields: μ_0H =0, 6 and 14 T. In addition to the moderate magnetoresistance, one can see that a weak insulating behavior is induced by the magnetic field. This weak semiconducting behavior is of course anti-intuitive for a normal state with Fermi liquid characteristic. A simple explanation would be that the insulating feature is given by an adjacent competing order here, once the superconductivity is suppressed, the latter is getting promoted. However, we should mention that the insulating behavior starts actually at 25 K (at 6 and 14 T) which is far beyond the SC transition temperature here. Someone may argue the minimum in the resistivity is caused by some impurities of Bi_2S_3, which shows a minima around 25 K[27], but this may be excluded because we do not see this phenomenon in zero magnetic field. Another possibility is that the conduction band has a very shallow band edge, as illustrated by the band structure calculations[26]. When a magnetic field is applied, the density of states (DOS) of the spin-up and spin-down electrons will become asym-
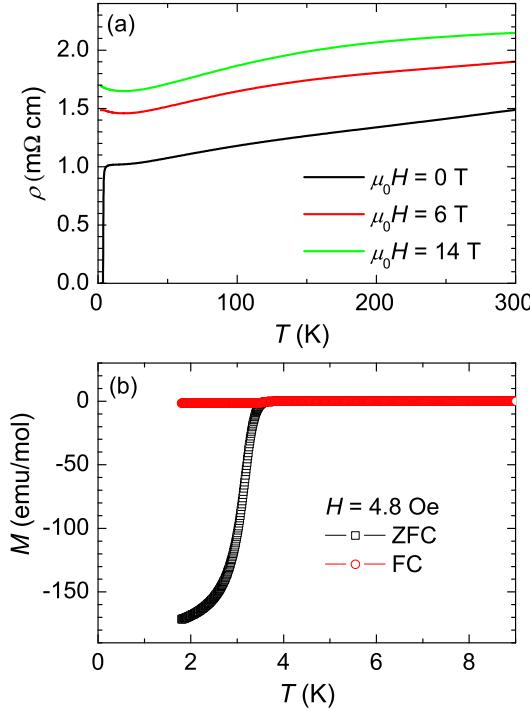
FIG. 2: (color online) (a) Temperature dependence of resistivity measured at three magnetic fields: $\mu_0 H = 0$, 6 and 14 T. It is clear that, beside a moderate magnetoresistance effect, a weak insulating behavior is induced by the magnetic field. (b) The temperature dependence of magnetization near the SC transition measured with $H = 4.8$ Oe in the field-cooled (FC) and zero-field-cooled processes (ZFC).

FIG. 3: (color online) (a) Temperature dependence of resistivity in $Bi_4O_4S_3$ at zero field near the resistive transition. The onset transition temperature T_c^{onset} at the crossing point of the normal state background (guided by a red dashed line) and the extrapolated line of the steep resistive transition part (guided by a blue dash-dot line) is 4.2 K. The resistance difference between the resistive curve and the normal state background extends to a very high temperature shown in the inset, which suggests that the SC fluctuation may be strong in this material. (b) An enlarged view for the temperature dependence of resistivity at magnetic fields of (from bottom to top) 0, 0.1 to 0.6 T with increments of 0.1 T; 0.8, 1, 1.5, 2 to 7 with increments of 1 T; and 9, 12, 14 T. It is found that the bulk superconductivity can be quickly suppressed by the magnetic field, while the onset transition temperature changes slightly, indicating a strong fluctuation effect. (c) Temperature dependence of the resistivity (as shown in (b)) normalized at 10 K. A kink can be clearly seen at about 4 K when the magnetic field is high and the bulk superconductivity is suppressed completely. The red arrowed line traces out the evolution from the SC onset transition in the low field region to a kink at high magnetic fields.

metric given by the Zeeman effect. Therefore we have some polarized electrons which induce the weak insulating behavior. Clearly this insulating behavior needs to be further checked, better with single crystals in the future, and to be explained satisfactorily. In Fig. 2(b) we present the magnetization data measured in the zero-field-cooled (ZFC) and the field-cooled mode (FC). The SC magnetic transition starts at about 3.6 K. Superconducting transition temperature in this paper is a little lower than that in previous report by Mizuguchi et al.[22], probably due to mutual doping between the O and S elements. From the resistive curve in the transition region as shown in Fig. 3(a), the critical temperature taken from 5% of the normal state resistivity (T_c^{zero} or T_{irr}) is 3.7 K. The onset transition temperature T_c^{onset} determined from the crossing point of the normal state line and the extrapolation of the steep transition line is about 4.2 K, while $T_c(99\%\rho_n)$ taken from the 99% of the normal resistance is about 6.2 K. It should be noted that the excess conductivity region in which the resistivity starts to deviate from the normal state line (inset of Fig. 3(a)) can extend to the temperature above 10 K. This excess conductiv-
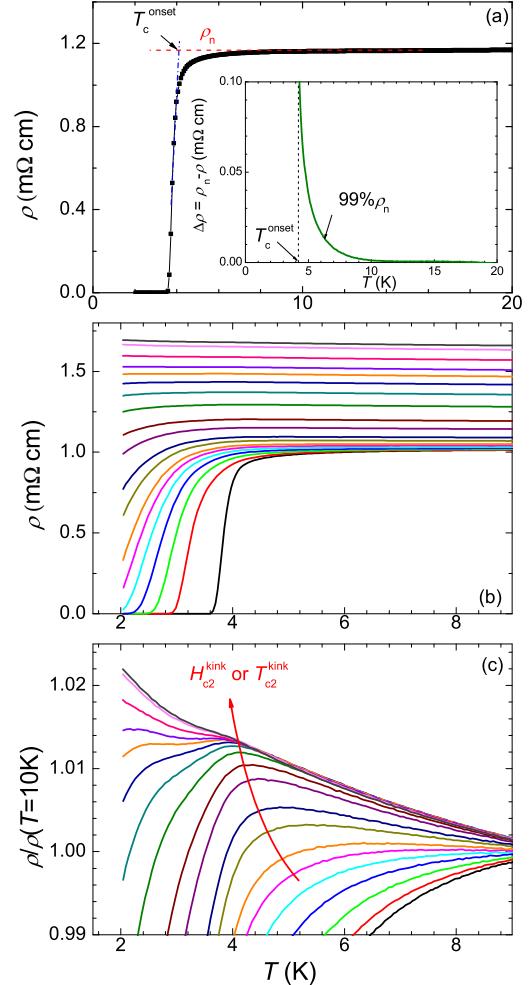
ity is usually regarded as the SC fluctuation from the residual Cooper pairs above bulk $T_c(99\%\rho_n)$. This superconducting fluctuation is actually expected by the band structure calculations which foresee a low dimensionality of the electronic structure, and can be corroborated by the quickly broadened resistive transition under magnetic fields, as shown in Fig. 3(b). One can see that the transition temperature with zero resistivity can be suppressed blow 2 K by a magnetic field as low as 0.4 T, while the bulk superconductivity is suppressed completely by a magnetic field of 5 T. However, even if the bulk superconductivity is easily suppressed, a kink appears on the ρ vs T curve at a high magnetic field where one cannot see the diamagnetization. If following the onset transition of the resistivity, as shown in Fig. 3(c), we can see that the kink has very close relationship with the upper critical field $\mu_0 H_{c2}$ in the low field and high temperature region. Because it is really difficult to define the temperature below which ρ_n first deviates from its high temperature behavior, we use these kink positions to define the upper critical fields above 1 T. Surprisingly, this kink stays at about 4 K even with a magnetic field of 14 T. We interpret this kink as the temperature below which the residual Cooper pairs exist in the system even the bulk superconductivity is completely suppressed. Following the tendency of this kink, a very high critical field can be expected in the zero temperature limit, which certainly exceeds the Pauli limit given by $\mu_0 H_p = 1.84 T_c$.[28]

To make further analysis on the superconducting property, we measured STS spectra on this sample. Several typical STS curves measured at 1.6 K below the bulk SC transition are shown in Fig. 4(a). Most of the spectra are symmetric with very clear suppression of DOS within a certain energy scale, and clear coherence peaks can be found on some spectra. However the coherence peaks on most of the curves are somewhat broad and the zero-bias conductance values are remarkably large, which maybe due to the contamination of the surface on this polycrystalline sample. The gap values determined from the coherence peaks or the kink position to the superconducting valleys (arrows in Fig. 4(a)) are mainly 3 meV for most of the spectra, while some of the spectra show much larger gap sizes or even two-gap features. In high-T_c superconductors, sometimes a bosonic mode which exhibits as a peak feature at a higher energy outside of the superconducting gap is found by STS measurements[29,30]. The second gap in $Bi_4O_4S_3$ resembles the bosonic mode feature. However such high-energy peaks are quite rare to occur in hundreds of measured spectra, so we just regard it as a possible second gap. In order to know the average value of the superconducting gap, we do the statistic analysis to the gap size Δ taken from 400 spectra and present in Fig. 4(b). One can see that the mean gap value $\overline{\Delta}$ is about 3 meV. Considering the bulk superconducting transition temperature T_c^{onset} of 4.2 K, we get the ratio $2\overline{\Delta}/k_B T_c \sim 16.6$, which is almost 5 times of the value given by the BCS theory in the weak coupling regime. It is even higher than the values of most high-T_c
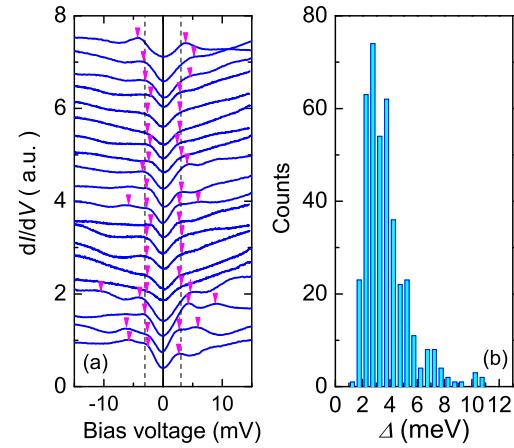

FIG. 4: (color online) (a) Typical tunnelling spectra measured at different locations on the polycrystalline samples. The gap values judged from the peaks or humps on the spectra are marked by the arrows. One can see that the mean gap value is around 3 meV as guided by the vertical dashed lines. Some spectra show very large gap values and even have two-gap features. (b) Statistics on the local SC gap sizes Δ of 400 spectra. The gap size follows the Gaussian distribution with the mean gap value $\overline{\Delta} = 3$ meV. Such a large gap value suggests the unconventional superconductivity in $Bi_4O_4S_3$ with $T_c^{onset} = 4.2$ K. The largest SC gap can reach a value of about 10 meV

superconductors. This suggests the very strong coupling superconductivity in the superconductor. Since the scattering is really strong in the polycrystalline sample, it is very difficult to judge the pairing symmetry from the fitting to the spectra. As shown in Fig. 4(b), the gap size can extend to a very large value, e.g., exceeding 10 meV. Such inhomogeneity of SC gap sizes needs to be verified by other experiment tools which may make it an interesting new material.

In Fig. 5(a), we show the temperature evolution of the STS spectra obtained by warming up the samples from 1.6 K through T_c to 20 K. One can see that the superconducting feature marked by the depression of the density of states near the Fermi energy persists at temperatures above the bulk $T_c(99\%\rho_n) \sim 6$ K. Such a feature disappeared at temperature above some fluctuation temperature $T_f = 14$ K leaving only a V-shaped background. If we use the spectrum measured at 20 K as the background, we can obtain the normalized curves at different temperatures as shown in Fig. 5(b). Superconducting feature is weakened with the increasing of temperature and evolve to a continuous background at the temperature above T_f. In traditional superconductors, the superconducting gapped features on tunnelling spectra vanish at the temperature just above T_c.[31] In contrast such feature in cuprates could exist at the temperature far beyond T_c, which has been regarded as the pseudo-
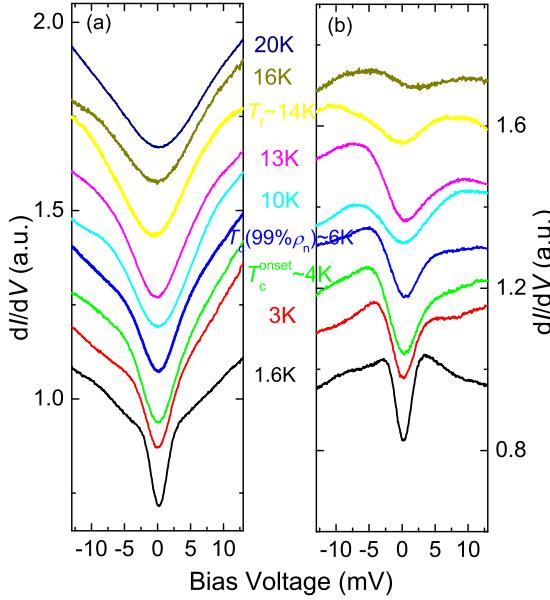
FIG. 5: (color online) (a) The evolution of the tunnelling spectra taken at temperatures from 1.6 K to 20 K. The spectra are displaced vertically for clarity. (b) The STS normalized by the one measured in normal state (at 20 K). One can see that the gapped feature vanishes at about 14 K which is much higher than the critical temperature for bulk superconductivity ($T_c(99\%\rho_n) \sim 6$ K), as shown by the blue curve.

gap effect[16]. Even in some iron pnictides, the gapped feature was observed to extend to a very high temperature[32] and was explained by the presence of possible pseudogap effect[33]. The pseudogap effect can also be observed from the kink in resistive curve in cuprates[13]. Because we cannot find any trace of pseudogap from the transport measurements, this effect at high temperature is supposed to be the SC fluctuation instead of the pseudogap. In addition, the estimation is consistent with excess conductivity at the temperature above bulk T_c. If using $T_f = 14$ K as the pairing temperature, we get the ratio $2\overline{\Delta}/k_B T_f \sim 5.0$ which is still a large value but comparable with the value calculated from the SC gap and the pseudogap temperature in cuprates[3]. It should be noted that some SC gap values could extend to very high, i.e., larger than 7 meV, which gives a much larger value of $2\overline{\Delta}/k_B T_f$. The detailed reason for this large energy gap remains unresolved.

Figure 6(a) shows the STS spectra taken at different magnetic fields at the same temperature 1.6 K. The bulk upper critical field $\mu_0 H_{c2}$ judged from the 99% of the normal state resistance at 1.6 K is about 5 T. The suppression to the DOS on the spectra are apparently without any variation when crossing this bulk transition temperature, and it is more clear for the normalized spectra by dividing out the background spectrum taken at 20 K and 0 T as shown in Fig. 6(b). As described above, the
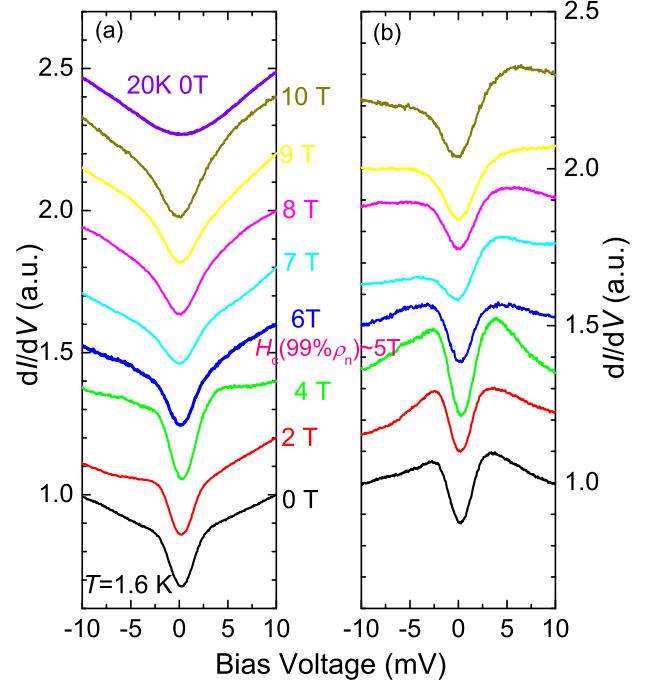

FIG. 6: (color online) (a) The evolution of the tunnelling spectra at different magnetic fields up to 10 T at 1.6 K. The spectra are displaced vertically for clarity. The spectrum taken at 20 K and 0 T is also shown for comparison. (b) The STS curves normalized by the one measured in normal state (at 20 K and 0 T). One can see the suppression of DOS remains at fields above the bulk upper critical field $H_c(99\%\rho_n) \sim 5$ T.

gapped feature on the spectra existing above $T_c(99\%\rho_n)$ is consistent with the picture of fluctuating superconductivity. Since the spectra at high magnetic fields are similar to those taken at zero field but at high temperatures, this suppression of DOS near Fermi energy observed above bulk $H_c(99\%\rho_n)$ can also be attributed to the SC fluctuation and preformed Cooper pairs.

III. DISCUSSION

Next we present a phase diagram based on the transport and STS measurements in Fig. 7 and give discussions on the possible mechanism of superconductivity. The SC transition point of critical field $H_c(99\%\rho_n)$ is shown by the red filled circles. The bulk superconductivity is established in a very small area covered by the irreversibility line T_{irr} (blue up-triangles). The large area between them indicates a strong SC phase fluctuation. This is actually consistent with the theoretical expectation because the electronic system has one dimensional feature(p_x and p_y). The bulk superconductivity is established between the one dimensional fluctuating superconducting chains. The curve marked with H_c^{onset} gives the upper critical
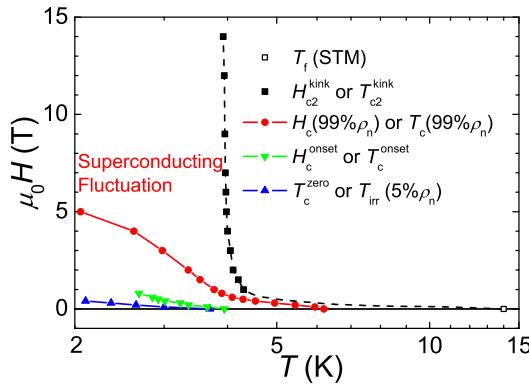
FIG. 7: (color online) Phase diagram derived from the resistive transition curves and the STS data. Semi-log plot is used to make the phase diagram more clear. The transition point judging from the 99% of the normal resistance gives rise to the upper critical field H_{c2}. The curve H_{c2}^{kink} shows the point determined from the kink point of the resistivity versus temperature which denotes the superconducting fluctuation property. Such fluctuation behavior with excess conductivity is proved by the STS data and extends to as high as 14 K at 0 T. The dashed line is a guide for eyes.

field determined using the usual crossing point of the normal state background and the extrapolated line of the steep resistive transition part. The most puzzling point is the kink appearing in the ρ vs. T data at a high magnetic field. The curve marked with H_{c2}^{kink} shows the critical field determined from the kinky point of the resistive data shown in Fig. 3(c), by following the trace of the arrowed red line there. We add the fluctuation temperature T_f from the tunnelling spectrum at zero magnetic field to the phase diagram, and get a wide fluctuation region at zero magnetic field. Since this line traces very well to the transition point marked by $H_c(99\%\rho_n)$ in the low field and high temperature region, we naturally attribute it to the existence of residual Cooper pairs. If this kink can be interpreted as the onset for the pairing, that would indicate a very strong pairing strength or gap, which can be inversely supported by the tunneling data. In a simple BCS picture, we have $H_{c2} = (\pi\Phi_0/2\hbar^2 v_F^2)\Delta^2$, where

Φ_0 is the flux quanta, v_F is the Fermi velocity. Such a strong pairing needs certainly a reasonable cause, which exceeds the limit of the simple phonon mediated pairing picture. By taking account of the weak correlation effect in the Bi 6p electrons, some other novel mechanism, such as the valence fluctuation of the Bi^{2+} and Bi^{3+}, may play an important role in this new superconductor.

IV. CONCLUSIONS

In summary, we perform the resistive and scanning tunnelling spectroscopy measurements on the new BiS_2 based superconductor $Bi_4O_4S_3$. A weak insulating behavior is induced in the normal state when a high magnetic field is applied. This can be induced either by an adjacent competing order, or the very shallow p_x and p_y band and small Fermi energy. A kink appears on the temperature dependence of resistivity at all high magnetic fields when the bulk superconductivity is completely suppressed. This kink can be regarded as the presence of local pairing, or the upper critical field $H_{c2}(T)$. The SC fluctuation region from the STS measurement extends to about 14 K although the bulk superconducting transition temperature is only about 3.7 K. The gapped feature near the Fermi energy can also extend to a high magnetic field (5 T), which is consistent with the resistive measurements, again indicating a strong superconducting fluctuation. From the tunnelling spectra, a mean superconducting gap of 3 meV is widely observed, which leads to a very high ratio of $2\Delta/k_B T_c \approx 16.6$, suggesting strong coupling superconductivity.

[†]huanyang@nju.edu.cn, [*]hhwen@nju.edu.cn

[1] Bednorz J G and Muller K A. Possible high T_c superconductivity in the Ba-La-Cu-O system. Zeitschrift fur Physik B Condensed Matter 1986, 64: 189-193

[2] Kamihara Y, Watanabe T, Hirano M, et al. Iron-Based Layered Superconductor La[$O_{1-x}F_x$]FeAs (x=0.05-0.12) with T_c=26 K. J. AM. CHEM. SOC 2008, 130: 3296-3297

[3] Fischer Ø, Kugler M, Maggio-Aprile I, et al. Scanning tunneling spectroscopy of high-temperature superconductors. Rev. Mod. Phys, 2007, 79: 353-419

[4] Hoffman J E. Spectroscopic scanning tunneling microscopy insights into Fe-based superconductors. Rep. Prog. Phys, 2011, 74: 124513

[5] Wolf E, Principles of Electron Tunneling Spectroscopy, Oxford University Press, New York, 1985

[6] Xu Z A, Ong N P, Wang Y, et al. Vortex-like excitations and the onset of superconducting phase fluctuation in underdoped $La_{2-x}Sr_xCuO4$. Nature(London), 2000, 406: 486-488

[7] Wang Y Y, Li L, Ong N P. Nernst effect in high-T_c superconductors. Phys. Rev. B, 2006, 73: 024510

8 Wang Y Y, Li L, Naughton M J, et al. Field-Enhanced Diamagnetism in the Pseudogap State of the Cuprate $Bi_2Sr_2CaCu_2O_{8+\delta}$ Superconductor in an Intense Magnetic Field. Phys. Rev. Lett, 2005, 95: 247002

9 Wen H H, Mu G, Luo H Q, et al. Specific-Heat Measurement of a Residual Superconducting State in the Normal State of Underdoped $Bi_2Sr_{2-x}La_xCuO_{6+\delta}$ Cuprate Superconductors. Phys. Rev. Lett, 2009, 103: 067002

10 Rourke P M C, Mouzopoulou I, Xu X F, et al. Phase-fluctuating superconductivity in overdoped $La_{2-x}Sr_xCuO_4$, Nature Physics, 2011, 7: 455-458

11 Zhu Z W, Xu Z A, Lin X, et al. Nernst effect of a new iron-based superconductor $LaO_{1-x}F_xFeAs$. New J. Phys, 2008, 10: 063021

12 Pourret A, Malone Liam, Antunes A B, et al. Strong correlation and low carrier density in $Fe_{1+y}Te_{0.6}Se_{0.4}$ as seen from its thermoelectric response. Phys. Rev. B, 2011, 83: 020504

13 Timusk T, Statt B. The pseudogap in high-temperature superconductors: an experimental survey. Rep. Prog. Phys, 1999, 62: 61-122

14 Kondo T, Hamaya Y, Palczewski A D, et al. Disentangling Cooper-pair formation above the transition temperature from the pseudogap state in the cuprates. Nature Physics, 2011, 7: 21-25

15 Grbić M S, Požek M, Paar D, et al. Temperature range of superconducting fluctuations above T_c in $YBa_2Cu_3O_{7-\delta}$ single crystals. Phys. Rev. B, 2011, 83: 144508

16 Renner C, Revaz M, Genoud J Y, et al. Pseudogap Precursor of the Superconducting Gap in Under- and Overdoped $Bi_2Sr_2CaCu_2O_{8+\delta}$. Phys. Rev. Lett, 1998, 80: 149-152

17 Anderson P W, Lee P A, Randeria M, et al. The physics behind high-temperature superconducting cuprates: the 'plain vanilla' version of RVB. J. Phys: Condens. Matter, 2006, 16: R755-R769

18 Scalapino D J. The case for $d_{x^2-y^2}$ pairing in the cuprate superconductors. Physics Report, 1995, 250:329-365. Moriya T, Ueda U. Antiferromagnetic spin fluctuation and superconductivity. Rep. Prog. Phys, 2003, 66: 1299-1341. Monthoux P, Pines D, Lonzarich G G. Superconductivity without phonons, Nature (London) 2007, 450: 1177-1183

19 Ni N, Tillman M E, Yan J Q, et al. Effects of Co substitution on thermodynamic and transport properties and anisotropic H_{c2} in $Ba(Fe_{1-x}Co_x)_2As_2$ single crystals. Phys. Rev. B, 2008, 78: 214515

20 Si Q M, Steglich F. Heavy Fermions and Quantum Phase Transitions. Science, 2010, 329: 1161-1166

21 Dressel M. Quantum criticality in organic conductors? Fermi liquid versus non-Fermi-liquid behaviour. J. Phys. Condens. Matter, 2011, 23: 293201

22 Mizuguchi Y, Fujihisa H, Gotoh Y, et al. BiS_2-based layered superconductor $Bi_4O_4S_3$. Phys. Rev. B, 2012, 86: 220510

23 Mizuguchi Y, Demura S, Deguchi K, et al. Superconductivity in Novel BiS_2-based superconductor $LaO_{1-x}F_xBiS_2$. J. Phys. Soc. Jpn, 2012, 81: 114725

24 Demura S, Mizuguchi Y, Deguchi K, et al. New member of BiS_2-based superconductor $NdO_{1-x}F_xBiS_2$. J. Phys. Soc. Jpn, 2013, 82: 033708

25 Xing J, Li S, Ding X X, et al. Superconductivity appears in the vicinity of semiconducting-like behaviour in $CeO_{1-x}F_xBiS_2$. Phys. Rev. B, 2012, 86: 214518

26 Usui H, Suzuki K, Kuroki K. Minimal electronic models for superconducting BiS_2 layers. Phys. Rev. B, 2012, 86: 220501(R)

27 Chen B X and Uher. Transport properties of Bi_2S_3 and the ternary bismuth sulfides $KBi_{6.33}S_{10}$ and $K_2Bi_8S_{13}$. Chem Matter, 1997, 9: 1655-1658

28 Clogston A M. Upper Limit for the Critical Field in Hard Superconductors. Phys. Rev. Lett, 1962, 9: 266-267

29 Niestemski F C, Kunwar S, Zhou S. A distinct bosonic mode in an electron-doped high-transition-temperature superconductor. Nature, 450: 1058-1061

30 Wang Z Y, Yang H, Fang D L, et al. Close relationship between superconductivity and the bosonic mode in $Ba_{0.6}K_{0.4}Fe_2As_2$ and $Na(Fe_{0.975}Co_{0.025})As$. Nature Physics 2013, 9: 42-48

31 Pan S H, Hudson E W and Davis J C. Vacuum tunneling of superconducting quasiparticles from atomically sharp scanning tunneling microscope tips. Appl. Phys. Lett, 1998, 73: 2992

32 Yang H, Wang Z Y, Fang D L, et al. Unexpected weak spatial variation in the local density of states induced by individual Co impurity atoms in superconducting $Na(Fe_{1-x}Co_x)As$ crystals revealed by scanning tunneling spectroscopy. Phys. Rev. B, 2012, 86: 214512

33 Zhou X D, Cai P, Wang A F, et al. Evolution from Unconventional Spin Density Wave to Superconductivity and a Pseudogaplike Phase in $NaFe_{1-x}Co_xAs$. Phys. Rev. Lett, 2012, 109: 037002